Acta Materialia 139 (2017) 215–225

Contents lists available at ScienceDirect

Acta Materialia

journal homepage: www.elsevier.com/locate/actamat

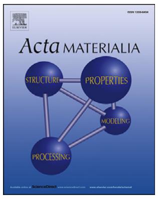

Full length article

Simultaneous determination of the lattice thermal conductivity and grain/grain thermal resistance in polycrystalline diamond

J. Anaya [a], T. Bai [b], Y. Wang [b], C. Li [b], M. Goorsky [b], T.L. Bougher [c], L. Yates [c], Z. Cheng [c], S. Graham [c], K.D. Hobart [d], T.I. Feygelson [d], M.J. Tadjer [d], T.J. Anderson [d], B.B. Pate [d], M. Kuball [a], *

[a] Center for Device Thermography and Reliability (CDTR), University of Bristol, Bristol BS8 1TL, United Kingdom
[b] Materials Science and Engineering, University of California Los Angeles, CA 90095, USA
[c] George W. Woodruff School of Mechanical Engineering, Georgia Institute of Technology, Atlanta, GA 30313, USA
[d] Naval Research Laboratory, 4555 Overlook Ave SW, Washington, DC 20375, USA

ARTICLE INFO

Article history:
Received 30 March 2017
Received in revised form
3 August 2017
Accepted 4 August 2017
Available online 9 August 2017

Keywords:
Thermal conductivity
Nanocrystalline diamond
Grain boundaries

ABSTRACT

The in-plane and cross-plane thermal conductivity of polycrystalline diamond near its nucleation region have been measured by Raman thermography assisted by TiO_2 nanoparticles and by picosecond time-domain thermoreflectance (TDTR). This information has been combined with a finite element thermal model making use of the real grain structure, including information on the grain orientation, of the film extracted by transmission electron microscopy (TEM). This methodology allows to simultaneously determine the thermal resistance between grains and the lattice thermal conductivity of the sample without any adjustable parameter. The results show that the lattice thermal conductivity of the near nucleation diamond is 5–8 times smaller than the one observed in IIa single-crystalline diamond; the thermal resistance between grains is at least one order of magnitude higher than values predicted by molecular dynamic simulations. Finally, we show how the anisotropy in thermal conductivity observed in polycrystalline diamond naturally emerges from its grain structure and the thermal resistance at grain boundaries.

1. Introduction

The high thermal conductivity of diamond (up to 3300 W/mK) has been widely exploited in thermal management of different applications, e.g. high power lasers [1], high power light emitting diodes (LEDs) [2], x-ray optical windows [3] and high power electronic devices [4]. In all of these applications, and because nowadays polycrystalline diamond can reach thermal conductivities approaching those of single crystal diamond, polycrystalline rather than single crystalline diamond is used without any detriment [5]. However, for achieving this performance polycrystalline diamond needs to be polished removing the material of the first microns of growth corresponding to the near nucleation diamond [6]. In this region, comprising the first microns of diamond from nucleation, the thermal conductivity is much lower than bulk values; it is also anisotropic i.e. cross-plane and in-plane thermal conductivity differ in value; the thermal conductivity also shows a strong dependence on the average grain size [6–8]. Due to the difficulty of measuring the thermal properties of ultra-thin diamond films, the thermal transport in this region of the diamond has been scarcely studied, and the existent data reported in the literature show significant disparity in values [8]. However, the recent integration of diamond with GaN high electron mobility transistors (HEMTs) has revived the interest in a better understanding of the diamond properties in this near-nucleation region, since a low thermal conductivity in this region may be a bottleneck for this technology [9–11]. It should be noted that the thermal conductivity values reported in the literature for ultrathin diamond layers (<3 μm) range from a few tens to few hundreds of W/mK [8,12–15], with cross plane/in-plane anisotropy rates ranging from 1.5 up to 20 [6,8,13–15]. To explain these low thermal conductivity values, two main factors have typically been considered: the low quality of the diamond lattice in this region, and the presence of grain boundaries acting as thermal barriers [6,8,13–15]. The latter has also been qualitatively used to

---

* Corresponding author.
E-mail address: martin.kuball@bristol.ac.uk (M. Kuball).

http://dx.doi.org/10.1016/j.actamat.2017.08.007
1359-6454/

justify the anisotropy in thermal conductivity due to the characteristic columnar shape of the polycrystalline diamond grains [6,8]. However, while these two factors undoubtedly impact the heat transport in the near nucleation diamond region, still it is poorly understood how to quantify their individual contribution to the reduction of thermal conductivity and how they are related to the emergence of anisotropy in the heat conduction.

Typically the quality of the lattice in polycrystalline diamond is typically explored by means of its Raman signal [16]. When approaching the near nucleation diamond it is common to observe features attributed to a low-quality lattice: the sp^3 diamond peak becomes broader than for single crystal/bulk CVD diamond, and other features appear in the Raman spectrum apart of the diamond Raman peak (sp^2 bonds, transpolyacetylene peaks, etc.) [16,17]. However, while this is clear evidence for a somewhat less crystalline lattice structure, it says little about whether these contributions to the Raman spectra arise from the in-grain lattice or from the grain boundaries regions, which are prone to accumulate defects including sp^2 and CH_x bonds [18,19]. On the other hand, theoretical values computed from molecular dynamics simulations have shown that the thermal resistance between perfect grain boundaries in polycrystalline diamond range between 0.02 and 0.1 m^2K/GW depending on its mismatch angle [20,21]. On the other hand, reported literature values for this magnitude from experimental measurements are much higher, on the order of 0.5–3 m^2K/GW [7,12,21], which can only be explained by a significant accumulation of defects/disorder at and near the grain boundaries [20]. It is worth noting that experimental values of grain/grain thermal resistance are typically extracted indirectly from experimental data. For this, models make use of strong simplifications, for example, bulk-like in-grain thermal conductivities [12,21] and a single average value for the in-plane grain size (in the case of the columnar grains those may be somewhat arbitrary due to the lack of regularity) are considered [8]. In any case, how the grain/grain thermal resistance correlates with the cross-plane thermal conductivity, and therefore the thermal conductivity anisotropy factor, is still poorly understood, and at best only approached by simplified models making use of indirect phenomenological relations [6].

To shed some light on this problem, we demonstrate in this work a methodology able to unravel the individual roles of grain boundaries and lattice thermal conductivity on the thermal transport in the near nucleation site of polycrystalline diamond. For this, we have determined the in-plane and cross-plane thermal conductivity experimentally in a polycrystalline diamond thin film (1 μm thick). This has been combined with thermal simulations making use of the real grain structure, including grain orientation, of the sample, which was determined by transmission emission microscopy (TEM). Using this methodology the in grain thermal conductivity and thermal resistance between grains can be simultaneously determined from both cross-plane and in-plane measurements without any fitting parameters.

2. Experimental details

Diamond films of about 1 μm thickness were deposited on 200 μm thick silicon substrates by microwave plasma-assisted chemical vapor deposition (MPCVD) in an IPLAS 5.0 KW CVD reactor with hydrogen and methane as reactant gases. The substrate temperature and chamber pressure were kept constant throughout the entire diamond film growth and remained at 750 °C and 7.08 torr respectively. The microwave power and methane to hydrogen ratio was varied, respectively, from 800 W to 0.5% during the initial 20 min of film growth to 1400 W and 0.7% through the continuing diamond deposition. The diamond film thickness was measured by in situ laser reflectometry. Prior to growth, the silicon substrate was seeded by ultrasonic treatment in ethanol-based nanodiamond suspension prepared from detonation nanodiamond powder which was acquired from International Technology Center, North Carolina, USA (ITC). According to the manufacturer specifications the material grade used here has a high degree of grain size homogeneity with an average particle size of 4 nm, and a chemical purity in excess of 98%. Scanning electron microscopy analysis (SEM) of the back side of a typical diamond film deposited with above mentioned seeding method shows a uniform nucleation with seed density greater than 10^{12} nuclei/cm^2. In general, the use of carbon-lean growth conditions is intended to suppress secondary renucleation, and increases film quality by decreasing grain/boundary ratio. Such diamond films are basically formed through the grain coalescence and subsequent growth competition of initially random oriented nanodiamond seeds. The orientation of crystallites fastest growth direction in relation to substrate surface is the key to seeds survival. Only the crystallites with fastest growth direction nearest to normal to the growth surface survive at the end. This ultimately leads to a formation of a well pronounced columnar grain structure in the film, as well as an increase in lateral grain size with film thickness.

The structural characterization included electron microscopy x-ray scattering techniques. Electron transparent plan view and cross section samples were prepared using a focused ion beam instrument (Nova 600 FIB). SEM images of the diamond surface morphology were also produced using the FIB instrument. Transmission electron microscopy (TEM) images were generated using a Titan S/TEM (FEI) system under 200 kV. The scanning transmission electron microscopy (STEM) mode allows to analyze the grain size distribution while the high angle annular dark field (HAADF) detector in the STEM mode provides contrast based on the differences in the adjacent grain orientation and distinguishes clearly between grain boundaries and twins. The orientation of the different grains was quantified using two techniques. First, selected area electron diffraction (SAED) patterns were used to produce images of grains with specific orientations. Tilting the sample imaged different grains, so the relative misorientation between adjacent grains could be estimated. The second approach was to employ precession electron diffraction (PED) mapping with a 10 nm step size from which the orientation of each grain is mapped using a color-coded legend. X-ray scattering measurements utilized a Jordan Valley D1 (CuK_α radiation) with incident parallel beam optics for both $2\theta:\omega$ scans and pole figures using Soller slits. Full pole figure data were collected with a fixed diffraction angle 2θ by varying the tilt angle with respect to the sample surface normal direction (χ) from 0° to 80° with a step size of 2° and rotation angle around sample surface normal direction (φ) from 0° to 360° with a step size of 1°. Pole figures were plotted with the obtained diffracted intensity data as a function of χ and φ.

For producing diamond membranes for in-plane thermal measurements, the silicon substrate was etched away by dry etching to obtain several 460 × 1000 μm freestanding diamond membranes similar to the ones described in Refs. [8,22]. Test structure designs consisted of metal heaters on these diamond membranes; this generates a temperature field in the freestanding diamond membrane when an electrical current flows through the line heater. The test structures were fabricated by first patterning 20 nm Cr followed by 300 nm Au by lift-off lithography. Diamond etching was performed by first depositing SiN by PECVD and patterning by ICP RIE using SF_6. Diamond was etched by RIE ICP O_2/Ar_2 chemistry. The SiN mask was removed by a combination of RIE ICP and buffered HF. Diamond membranes were fabricated by Bosch etching of the Si wafer to produce deep vias stopping selectively on the diamond film.